Available online at www.sciencedirect.com
SCIENCE DIRECT®
Journal of Magnetic Resonance 170 (2004) 56–66
JMR Journal of Magnetic Resonance
www.elsevier.com/locate/jmr

Effects of permeable boundaries on the diffusion-attenuated MR signal: insights from a one-dimensional model

A.L. Sukstanskii,[a,*] D.A. Yablonskiy,[a,b] and J.J.H. Ackerman[a,c,d]

[a] Department of Radiology, Biomedical MR Laboratory, Washington University, One Brookings Drive, St. Louis, MO 63130, USA
[b] Department of Physics, Biomedical MR Laboratory, Washington University, One Brookings Drive, St. Louis, MO 63130, USA
[c] Department of Chemistry, Biomedical MR Laboratory, Washington University, One Brookings Drive, St. Louis, MO 63130, USA
[d] Department of Internal Medicine, Biomedical MR Laboratory, Washington University, One Brookings Drive, St. Louis, MO 63130, USA

Received 6 April 2004
Available online 6 July 2004

Abstract

The local magnetization distribution $M(x,t)$ and the net MR signal S arising from a one-dimensional periodic structure with permeable barriers in a Tanner–Stejskal pulsed-field gradient experiment are considered. In the framework of the narrow pulse approximation, the general expressions for $M(x,t)$ and S as functions of diffusion time and the bipolar field gradient strength are obtained and analyzed. In contrast to a system with impermeable boundaries, the signal S as a function of the b-value is modeled well as a bi-exponential decay not only in the short-time regime but also in the long-time regime. At short diffusion times, the local magnetization $M(x,t)$ is strongly spatially inhomogeneous and the two exponential components describing S have a clear physical interpretation as two "population fractions" of the slow- and fast-diffusing quasi-compartments (pools). In the long-diffusion time regime, the two exponential components do not have clear physical meaning but rather serve to approximate a more complex functional signal form. The average diffusion propagator, obtained by means of standard q-space analysis procedures in the long-diffusion time regime is explored; its structure creates the deceiving appearance of a system with multiple compartments of different sizes, while in reality, it reflects the permeable nature of boundaries in a system with multiple compartments all of the same size.

Keywords: Diffusion; Magnetic resonance; Diffusion MRI; Membrane permeability; q-Space imaging

1. Introduction

It is well known that the presence of barriers leads to a non-mono-exponential b-value dependence of diffusion-attenuated MR signal. In numerous MR studies in biological systems, this dependence can be modeled well by a bi-exponential function with two different diffusion coefficients (large/fast and small/slow). The two exponential components are often ascribed to two physical compartments (typically, the extra- and intracellular spaces) in tissue. (For example, see the special issue of *NMR in Biomedicine* [1] and numerous references therein.)

We recently reported another possible origin of the "bi-exponentiality" of the diffusion-attenuated MR signal [2]. It was shown that the b-value dependence of diffusion-attenuated MR signal from a single compartment with an impermeable boundary in a Tanner–Stejskal pulse-field gradient experiment could also be approximated to a remarkable degree by a bi-exponential function at short diffusion time $t \ll t_D$, where $t_D = a^2/D_0$ is the "characteristic diffusion time" (a is a compartment size, D_0 is the free-diffusion coefficient). The physical underpinning of this approximation is the presence of a gradient-induced strongly inhomogeneous distribution of local transverse magnetization $M(x,t)$ at $t \ll t_D$. For cells of micron size, $t_D \sim 1$ ms, whereas most MR diffusion studies on humans and animals are usually performed with diffusion times much longer than 1 ms. Therefore this short-t mechanism of

* Corresponding author. Fax: 1-314-362-0526.
E-mail address: alex@wuchem.wustl.edu (A.L. Sukstanskii).

1090-7807/$ - see front matter © 2004 Elsevier Inc. All rights reserved.
doi:10.1016/j.jmr.2004.05.020

"bi-exponentiality" is relevant only for rather large cells such as the giant squid axon with diameter $\sim 300\,\mu m$ [3].

In the long-diffusion time regime, $t \geqslant t_D$, the bi-exponential behavior of the diffusion-attenuated MR signal can, in some cases, obviously be related to the tissue compartmentalization or a geometrical structure. However, in other cases, the origin of "bi-exponentiality" remains "mysterious" [4]. In particular, the fractional amplitudes of fast and slow diffusion components found by bi-exponential modeling of experimental data do not coincide with the known volume fractions of extra- and intracellular spaces. Here it is likely that a bi-exponential function simply describes the complex signal decay behavior better than does a mono-exponential function. Thus, there is no simple relationship between the bi-exponential model's amplitudes and decay rate constants and the physical parameters describing the microstructure of the structure under investigation. This point was clearly demonstrated in [5] by means of computer simulations. A general theoretical approach based on a statistical consideration that takes into account the diversity of tissue microstructure was developed in [6]. Experimentally, this point was also demonstrated in [7].

In the present paper, we demonstrate that bi-exponential behavior of the diffusion-attenuated MR signal in both short- and long-diffusion time regimes can be observed in a simple system with identical compartments separated by permeable boundaries (membranes). In the short-diffusion time regime, the physical origin of "bi-exponentiality" is the same as in the one-compartment model with impermeable boundaries [8], an inhomogeneous distribution of the transverse magnetization (the finite permeability of the boundaries μ leads only to quantitative variations in bi-exponential parameters). However, in the long-diffusion time regime, the permeability of the boundaries plays the major role defining bi-exponential signal decay behavior.

Development of a quantitative description of pulse-field gradient MR signal formation in multi-compartment systems with impermeable barriers between compartments in biological and porous media has been the subject of numerous studies, in which different approaches have been exploited. Generally, the local magnetization satisfies the well-known Bloch–Torrey equation [9] with appropriate boundary conditions. However, an analytical (or "close-to-analytical") solution to this equation can be found only for compartmental arrangements of the simplest geometry [8,10]. To the best of our knowledge, no analytical solution to the Bloch–Torrey equation is known for a system with permeable boundaries, and therefore numerical calculations and/or approximations are needed. In particular, the narrow pulse approximation has been used for an analysis of the MR signal in a one-dimensional periodic structure with permeable barriers [11] and in a system containing a sphere with permeable surface [12,13]. Numerous reports have been devoted to computer (Monte-Carlo) simulations or finite difference numerical solutions of the diffusion or Bloch–Torrey equations that make it possible to describe the MR signal in rather complicated multi-compartment structures [5,14–17]. A phenomenological approach based on introducing residence or pre-exchange lifetimes of the magnetization in compartments (two-site Kärger model and its three- and multi-site generalizations) has been developed in [18–23]. At long diffusion times, when a multi-compartment system can be characterized by a time-independent apparent diffusion coefficient (ADC), $\overline{D}$, different theoretical models have been examined in [14,21,24].

Practically all these studies describe the net MR signal in the system under consideration, whereas the local magnetization distribution has been discussed only recently [2,5,8]. A description of the time and spatial evolution of the local magnetization provides new insights into understanding of MR signal formation, as compared to a description of the net signal alone. In the present report, we describe the local magnetization distribution and the net signal in a multi-compartment system that allows a rather simple analytical solution in the narrow pulse approximation. This system is the one-dimensional, infinite, periodic structure with permeable barriers between compartments. The net MR signal in such a system was first considered by Tanner [11]. As noted in [14,24], this model leads to overemphasizing the influence of barriers that would be observed in real multi-barrier structures. This is because spin diffusion is "stopped" at long times by the model system's barriers (if the permeability tends to zero) and, thus, $\overline{D} \to 0$. In contrast, for real three-dimensional situations, e.g., in biological systems, spins can diffuse around compartments, e.g., cells, and, therefore, $\overline{D}$, determined by tortuosity, remains finite. Nevertheless, we adopt this simple model because the mathematical approach proposed here makes it possible to obtain rather simple expressions for the distribution of local magnetization and the net signal, allowing informative analyses in some practically important limiting cases. Besides, the model provides the correct behavior for an arbitrary system at short times when long trajectories (around compartments) can be ignored. In this regime, the time dependence of ADC is determined by a surface-to-volume ratio and is in agreement with a general expression obtained in [25].

2. General solution

Let us consider a uniform initial spin distribution contained in a one-dimensional infinite periodic structure consisting of compartments of size a separated by

non-absorbing and non-depolarizing boundaries (interfaces) of permeability μ. We consider a standard Stejskal–Tanner experiment with a pulse sequence composed of a 90° RF pulse followed by two compensated gradient pulses of strength G and duration δ placed symmetrically about a 180° RF refocusing pulse and separated by diffusion time t. The field gradient is applied along the normal to the boundaries. Note that for mathematical convenience, we use in this paper a notation t for the diffusion time (an interval separating the gradient pulses) rather than a more frequently used notation Δ.

For a one-dimensional system of arbitrary structure, the resulting net MR spin echo signal normalized to its initial value in the narrow pulse approximation [26,27] can be written as

$$S = \int_{-\infty}^{\infty}\int_{-\infty}^{\infty} \mathrm{d}x\,\mathrm{d}x_0 \exp(\mathrm{i}q(x_0 - x))\rho(x_0)\,P(x, x_0, t), \qquad (1)$$

where $q = \gamma G\delta$, γ is the magnetogyric ratio and $\rho(x_0)$ is the initial spin distribution. The signal S explicitly depends on the diffusion time t and the parameter q; for brevity, the arguments in S will be suppressed throughout the paper. The propagator $P(x, x_0, t)$ defining the probability for a spin to diffuse from a point x_0 to a point x during diffusion time t, satisfies the diffusion equation

$$\frac{\partial P}{\partial t} = D_0 \frac{\partial^2 P}{\partial x^2}, \qquad (2)$$

where D_0 is the diffusion coefficient in the absence of restrictive boundaries, i.e., D_0 is the "free"-diffusion coefficient. Eq. (2) is subject to the initial condition

$$P(x, x_0, 0) = \delta(x - x_0) \qquad (3)$$

and, introducing the specific one-dimensional model under consideration, to boundary conditions on the interfaces located at points $x = na$. A general solution to Eq. (2) is a piecewise function. Denoting the latter in the nth compartment, $(n-1)a \leqslant x \leqslant na$, as $P_n(x, x_0, t)$, the boundary conditions can be written in the form

$$\frac{\partial P_{n-1}}{\partial x} = \frac{\partial P_n}{\partial x}, \qquad D_0 \frac{\partial P_n}{\partial x} = \mu(P_n - P_{n-1}) \quad \text{at } x = na. \qquad (4)$$

The particular case $\mu = \infty$ correspond to free diffusion, the case $\mu = 0$ corresponds to completely impermeable boundaries.

In [11], the piecewise propagator $P(x, x_0, t)$ was found in the form of an eigenfunction expansion for the case of a finite number N of compartments, eigenvalues of the problem being calculated numerically (for a periodic system with infinite N, this procedure is obviously impossible). As mentioned in Section 1, this cumbersome numerical evaluation of eigenvalues did not take advantage of the periodicity of the system because the propagator $P(x, x_0, t)$ depends on the initial position x_0 and is an aperiodic function. The expression for the net signal found in [11] is essentially impossible to explore analytically and only numerical results for the propagator and, as a consequence, for the signal are available. In what follows, we use another approach based on deriving an equation directly for the local magnetization $M(x, t)$.

In the narrow pulse approximation adopted here, the local transverse magnetization can be found simply by removing the integration over x in Eq. (1):

$$M(x, t) = \int_{-\infty}^{\infty} \mathrm{d}x_0 \exp(\mathrm{i}q(x_0 - x))\rho(x_0)P(x, x_0, t). \qquad (5)$$

By making use of Eqs. (2)–(4), it can be readily verified that the function $M(x, t)$ satisfies Eq. (6)

$$\frac{\partial M}{\partial t} = D_0\left(\frac{\partial^2 M}{\partial x^2} + 2\mathrm{i}q\frac{\partial M}{\partial x} - q^2 M\right) \qquad (6)$$

with the initial condition

$$M(x, 0) = \rho(x). \qquad (7)$$

For a uniform initial spin distribution, $\rho(x) = 1$, the local magnetization is a periodic function of the coordinate x, $M(x, t) = M(x + a, t)$, which follows from an obvious property of the propagator in the periodic structure of period a: $P(x, x_0, t) = P(x + a, x_0 + a, t)$.

The local magnetization $M(x, t)$ is also a piecewise function of x. Denoting a solution to Eq. (6) in the nth compartment, $(n-1)a \leqslant x \leqslant na$, as $M_n(x, t)$, the boundary conditions at the interfaces can be written in the form:

$$\begin{aligned} &\frac{\partial M_n}{\partial x} + \mathrm{i}qM_n = \frac{\partial M_{n-1}}{\partial x} + \mathrm{i}qM_{n-1}, \\ &D_0\left(\frac{\partial M_n}{\partial x} + \mathrm{i}qM_n\right) = \mu(M_n - M_{n-1}) \end{aligned} \quad \text{at } x = na \qquad (8)$$

The Laplace transformation of the functions $M_n(x, t)$,

$$m_n(x, p) = \int_0^{\infty} \mathrm{d}t\, M_n(x, t)\exp(-pt), \qquad (9)$$

satisfies the ordinary differential equation (hereafter we consider $\rho(x) = 1$)

$$\frac{\partial^2 m_n}{\partial \tilde{x}^2} + 2\mathrm{i}\tilde{q}\frac{\partial m_n}{\partial \tilde{x}} - (\tilde{q}^2 + \kappa^2)m_n = -1 \qquad (10)$$

with the boundary conditions

$$\begin{aligned} &m_n' + \mathrm{i}\tilde{q}m_n = m_{n-1}' + \mathrm{i}\tilde{q}m_{n-1}, \\ &m_n' + \mathrm{i}\tilde{q}m_n = \tilde{\mu}(m_n - m_{n-1}) \quad \text{at } \tilde{x} = n. \end{aligned} \qquad (11)$$

Here we introduce dimensionless variables $\tilde{x} = x/a$, $\tilde{q} = qa$, $\kappa = (p/D_0)^{1/2}a$, and $\tilde{\mu} = \mu a/D_0$; a prime denotes a derivative with respect to $\tilde{x}$. As the local magnetization is a periodic function, $m_n(\tilde{x}, p) = m_{n-1}(\tilde{x} - 1, p)$, the boundary conditions (11) can be re-written in the form containing only the function $m_n(x, p)$:

$$m_n'(n-1,p)+\mathrm{i}\tilde{q}m_n(n-1,p)=m_n'(n,p)+\mathrm{i}\tilde{q}m_n(n,p),$$
$$m_n'(n,p)+\mathrm{i}\tilde{q}m_n(n,p)=\tilde{\mu}[m_n(n,p)-m_n(n-1,p)]. \tag{12}$$

A solution of Eq. (10) has the form:

$$m_n(\tilde{x},p)=A_n\exp(\lambda_1\tilde{x})+B_n\exp(\lambda_2\tilde{x})+C, \tag{13}$$

where

$$\lambda_{1,2}=-\mathrm{i}\tilde{q}\pm\kappa,\quad C=(\kappa^2+\tilde{q}^2)^{-1}. \tag{14}$$

The coefficients A_n and B_n are readily determined from the boundary conditions (12):

$$\begin{aligned}A_n&=-\frac{\mathrm{i}qC}{v}(\exp(\lambda_2)-1)\exp(-\lambda_1(n-1)),\\ B_n&=-\frac{\mathrm{i}qC}{v}(\exp(\lambda_1)-1)\exp(-\lambda_2(n-1)),\\ v&=\kappa(\exp(\lambda_2)-\exp(\lambda_1))\\ &\quad+2\tilde{\mu}(\exp(\lambda_1)-1)(\exp(\lambda_2)-1).\end{aligned} \tag{15}$$

Substituting Eqs. (14) and (15) into Eq. (13), we get

$$m(\tilde{x},p)=\frac{1}{(\kappa^2+\tilde{q}^2)}+\frac{\mathrm{i}\tilde{q}\exp(-\mathrm{i}\tilde{q}\tilde{x})}{(\kappa^2+\tilde{q}^2)}\times\frac{[\cosh(\kappa(1-\tilde{x}))-\exp(\mathrm{i}\tilde{q})\cosh(\kappa\tilde{x})]}{[2\tilde{\mu}(\cosh\kappa-\cos\tilde{q})+\kappa\sinh\kappa]}. \tag{16}$$

Hereafter we write down the magnetization distribution only in the compartment $0\leqslant\tilde{x}\leqslant 1$ ($n=1$), omitting the subscript n; due to periodicity of the magnetization distribution, the function $m_n(\tilde{x},p)$ in the nth compartments is given by Eq. (16) with the substitution $\tilde{x}\to\tilde{x}-n+1$. The Laplace transform of the net signal (per unit length), $s(p)$, can be found by integrating Eq. (16) over $\tilde{x}$ within the interval $[0,1]$:

$$s(p)=\frac{1}{(\kappa^2+\tilde{q}^2)}+\frac{2\tilde{q}^2}{(\kappa^2+\tilde{q}^2)^2}\times\frac{(\cosh\kappa-\cos\tilde{q})}{[2\tilde{\mu}(\cosh\kappa-\cos\tilde{q})+\kappa\sinh\kappa]}. \tag{17}$$

In the time domain, the magnetization $M(x,t)$ and the net signal (per unit length) $S(t)$ are determined by the inverse Laplace transformation of Eqs. (16) and (17). Using Mellin's formula, the functions $M(x,t)$ and $S(t)$ are, after some algebra, of the form:

$$M(x,t)=2\mathrm{i}\tilde{q}\sum_j\frac{\exp(-k_j^2\tau)\exp(-\mathrm{i}qx)[\cos(k_j(1-x/a))-\exp(\mathrm{i}\tilde{q})\cos(k_jx/a)]}{(\tilde{q}^2-k_j^2)[(2\tilde{\mu}+1)\sin k_j+k_j\cos k_j]}, \tag{18}$$

$$S=\frac{2\tilde{q}^2}{\tilde{\mu}}\sum_j\frac{\exp(-k_j^2\tau)k_j^2\sin k_j}{(\tilde{q}^2-k_j^2)^2[(2\tilde{\mu}+1)\sin k_j+k_j\cos k_j]}, \tag{19}$$

where $\tau=t/t_{\mathrm{D}}$, $t_{\mathrm{D}}=a^2/D_0$ is the characteristic diffusion time; the sums in Eqs. (18) and (19) are over all non-negative roots k_j of the transcendental equation

$$2\tilde{\mu}(\cos k-\cos\tilde{q})-k\sin k=0. \tag{20}$$

Note that the roots periodically depend on the parameter $\tilde{q}$, and, for their analysis, it is sufficient to consider $0<\tilde{q}\leqslant\pi$. In the case of small reduced permeability, $\tilde{\mu}\ll 1$, all the roots are close to $j\pi$:

$$\begin{aligned}k_0&\simeq 2\tilde{\mu}^{1/2}\sin\frac{\tilde{q}}{2},\quad j=0,\\ k_j&\simeq j\pi+\frac{2\tilde{\mu}}{j\pi}[1-(-1)^j\cos\tilde{q}],\quad j\geqslant 1.\end{aligned} \tag{21}$$

In the opposite case of high permeability, $\tilde{\mu}\gg 1$, the roots are approximately equal to

$$k_j\simeq(2j\pi\pm\tilde{q})\left(1-\frac{1}{2\tilde{\mu}}\right). \tag{22}$$

It follows from Eq. (18) that $M((n+1/2)a-x,t)=M^*((n+1/2)a+x,t)$ and thus the real part of the local magnetization is a symmetric function whereas the imaginary part is an antisymmetric function of the coordinate x with respect to the center of each compartment. As a consequence, only the real part of local magnetization contributes to the net signal. Note also that $\mathrm{Re}\,M$ is continuous on the boundaries whereas $\mathrm{Im}\,M$ has a discontinuity. As an example, Fig. 1 illustrates a distribution of the real (A) and imaginary (B) parts of the local magnetization $M(x,t)$ in the periodic structure at short diffusion time $t\ll t_{\mathrm{D}}$ ($\tau\ll 1$).

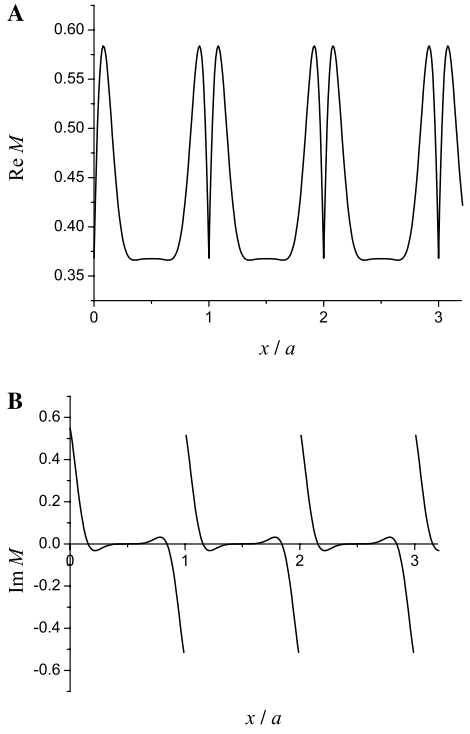

Fig. 1. The real (A) and imaginary (B) parts of the local magnetization in the periodic structure ($\tau=0.01$, $\tilde{\mu}=0.5$).

3. Results and discussion

In the limiting case of *free diffusion* ($\mu = \infty$), expressions for $M(x,t)$ and S are easier to obtain directly from the Laplace transform (16). In this limit, the second terms in Eqs. (16) and (17) vanish, and the inverse Laplace transformation of the first terms immediately leads to a homogeneous local magnetization distribution M and to the well-known result for the net signal in the case of unrestricted diffusion [27]:

$$S = \exp(-bD_0), \tag{23}$$

where the b-value for the narrow pulse approximation is equal to

$$b = q^2 t. \tag{24}$$

In the opposite limit of completely *impermeable boundaries* ($\mu = 0$), the roots of Eq. (20) are $k_j = j\pi$, $j = 0, 1, 2, \ldots$, and Eqs. (18) and (19) reduce to

$$M(x,t) = \mathrm{i}\mathrm{e}^{-\mathrm{i}qx}\left\{\frac{1-\mathrm{e}^{\mathrm{i}\tilde{q}}}{\tilde{q}} + 2\tilde{q}\sum_{j=1}^{\infty}\frac{\exp(-\pi^2 j^2\tau)\cos(\pi jx/a)[1-(-1)^j\mathrm{e}^{\mathrm{i}\tilde{q}}]}{(\tilde{q}^2-\pi^2 j^2)}\right\}, \tag{25}$$

$$S(t) = \frac{2(1-\cos\tilde{q})}{\tilde{q}^2} + 4\tilde{q}^2\sum_{j=1}^{\infty}\frac{\exp(-\pi^2 j^2\tau)[1-(-1)^j\cos\tilde{q}]}{(\tilde{q}^2-\pi^2 j^2)^2}. \tag{26}$$

Expression (26) coincides with the well-known result [28] for the net MR signal in a single compartment with impermeable boundaries.

Eqs. (18) and (19) make it possible to calculate the local magnetization distribution and the net signal for arbitrary values of permeability μ. In Fig. 2A we show the real part of the local magnetization distribution, $\mathrm{Re}\,M$, within a single compartment, calculated on the basis of Eq. (18) at different diffusion times $\tau = t/t_D$ for fixed values of reduced permeability $\tilde{\mu} = 0.5$ and b-value, $bD_0 = 1$. At a very short diffusion time $\tau = 0.01$ (line 1), there are two clearly distinguished maxima located close to the boundaries (edge enhancement effect) and a substantial area in the central part of the system where $\mathrm{Re}\,M$ is small and uniform. Note that an absolute value of the local magnetization, $|M(x,t)|$, has maxima directly on the boundaries whereas the maxima of $\mathrm{Re}\,M$ are slightly shifted from them. The magnetization in the central part of the compartment, where diffusion can be considered as almost unrestricted, is largely determined by the b-value: $\mathrm{Re}\,M \simeq \exp(-bD_0) \approx 0.368$ for $bD_0 = 1$. For a longer time, $\tau = 0.05$ (line 2), the maxima become broader and the region of uniform magnetization in the central part of the compartment disappears. At $\tau = 0.1$ (line 3), the maxima merge. It is interesting to note that the value of $\mathrm{Re}\,M$ at the boundaries ($x = 0$ and $x = a$) at $\tau \leqslant 0.1$ is also determined mainly by the b-value and is described by the free-diffusion expression $\mathrm{Re}\,M(x = 0, t) \simeq \exp(-bD_0)$ (see below Eq. (30)). However, for longer diffusion time ($\tau = 0.5$, line 4), $\mathrm{Re}\,M$ at the boundaries becomes already substantially different from its free-diffusion value and increases with time. At $\tau > 1$, $\mathrm{Re}\,M$ is practically uniform everywhere and gradually increases with diffusion time (motional narrowing regime).

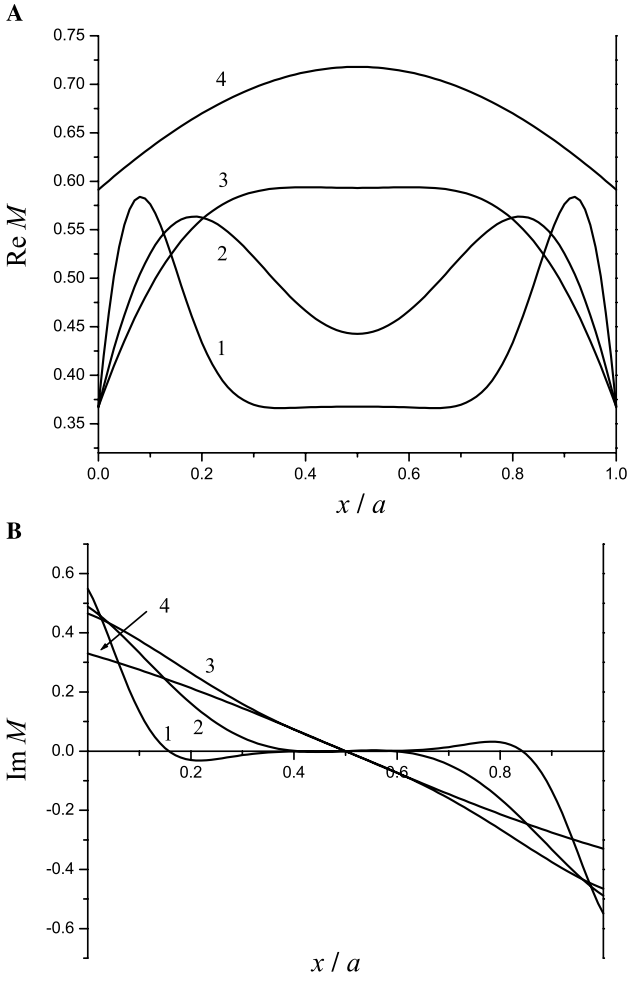

Fig. 2. The real (A) and imaginary (B) parts of the local magnetization in a single period of the periodic structure for different diffusion times $\tau = t/t_D$: 1, $\tau = 0.01$; 2, $\tau = 0.05$; 3, $\tau = 0.1$; and 4, $\tau = 0.5$. The reduced permeability and the b-value are fixed, $\tilde{\mu} = 0.5$, $bD_0 = 1$.

The antisymmetric (with respect to the compartment's center) imaginary part of the local magnetization, $\mathrm{Im}\,M$, is shown in Fig. 2B for the same diffusion times and $\tilde{\mu} = 0.5$, $bD_0 = 1$. For $\tau \leqslant 0.05$, $\mathrm{Im}\,M$ is close to 0 in the center part and achieves its extremal values at the boundaries. For $\tau \geqslant 0.1$, the uniform central part disappears and $\mathrm{Im}\,M$ is practically a linear function of x, a slope decreasing as diffusion time increases. In the motional narrowing regime, $\tau > 1$, the imaginary part of the local magnetization is negligibly small, $\mathrm{Im}\,M \simeq 0$.

Fig. 2 illustrates the local magnetization for a fixed reduced permeability $\tilde{\mu} = 0.5$. As the permeability decreases, the maxima in $\mathrm{Re}\,M$ at short times increase and for $\tilde{\mu} < 0.1$, the local magnetization becomes practically independent of $\tilde{\mu}$. In the motional narrowing regime, $\mathrm{Re}\,M$ increases as permeability decreases.

Simple analytical expressions for the signal can be obtained in the short-diffusion time regime, when $t \ll t_D$ ($\tau \ll 1$), and in the long-diffusion time regime, when $t \gg t_D$ ($\tau \gg 1$).

3.1. Short-diffusion time regime

In the short-diffusion time regime, $t \ll t_D$, the sum in Eqs. (18) and (19) converges rather slowly. To obtain an explicit expression for the time dependence of the signal in this regime, it is more convenient first to expand the Laplace transform $s(p)$ for large $|p| \gg 1$,

$$s(p) \simeq \frac{1}{p+\tilde{q}^2} + \frac{2\tilde{q}^2}{(p+\tilde{q}^2)^2(\kappa+2\tilde{\mu})}, \quad |p| \gg 1 \tag{27}$$

and then use the inverse Laplace transformation. An explicit analytical expression for the signal $S(t)$ in the short-diffusion time regime $t \ll t_D$, is given in Appendix A. This expression can be further simplified if the following conditions are also met: $t \ll t_D/(qa)^2$ and $t \ll D_0/4\mu^2$:

$$S(t) \simeq 1 - \overline{D}(t)\, q^2 t,$$
$$\overline{D}(t) \simeq D_0\left[1 - \frac{8}{3\pi^{1/2}}\frac{(D_0 t)^{1/2}}{a} - \frac{q^2 D_0 t}{2} + 2\frac{\mu t}{a} + \mathrm{O}(t^{3/2})\right]. \tag{28}$$

In Eq. (28) a time-dependent ADC $\overline{D}(t)$ is introduced. The first three terms in the function $\overline{D}(t)$ are similar to those in a short-diffusion time expansion of the ADC in the system with impermeable boundaries; in particular, the second term is a one-dimensional analog of a "surface-to-volume" term found in [25]. The term proportional to μ describes a contribution to $\overline{D}(t)$ related to the finite permeability of the boundaries. The permeability contribution to the ADC $\overline{D}(t)$ at short times is small as compared to the surface-to-volume term as was previously noted in [24]. Obviously, however, for high permeability, the approximate expression (28) takes place only at very short diffusion time and is completely invalid in the limit of free diffusion, $\mu \to \infty$.

The local magnetization distribution at short times can also be obtained in an analytical form in the similar manner. In particular, at the boundaries ($x = 0$), the expansion of the Laplace transform of the local magnetization $m(x = 0, p)$ at $|p| \gg 1$ has the form:

$$m(x=0,p) \simeq \frac{1}{p+\tilde{q}^2} + \frac{\mathrm{i}\tilde{q}}{(p+\tilde{q}^2)(2\tilde{\mu}+\kappa)}, \quad p \gg 1. \tag{29}$$

The inverse Laplace transformation of Eq. (29) leads to

$$M(x=0,t) = \exp(-D_0 q^2 t) + \mathrm{i}qaI_1(qa,\mu,t) \quad t \ll t_D, \tag{30}$$

where $I_1(qa,\mu,t)$ is a real function of its arguments (it is given in Appendix A). It is worth noting that, according to Eq. (30), the quantity $\mathrm{Re}[M_n(x=0,t)]$ is independent of the permeability and its time dependence is described by the expression characteristic to the free diffusion.

As shown in [2] for the model with impermeable boundaries, at short times, $t \ll t_D$, when the spatial distribution of the local magnetization is strongly inhomogeneous and the quasi-two-compartments can be distinguished, the net signal as a function of the b-value, $b = q^2 t$, can be extremely well approximated by the bi-exponential function (diffusion time t is fixed)

$$S_b = \zeta \exp(-bD_1) + (1-\zeta)\exp(-bD_2), \tag{31}$$

where ζ is the "volume fraction" of the spins near the boundaries. A physical explanation of this is given in [2]. At $t \ll t_D$, all spins can be conditionally divided into two populations: one population, comprising spins located far from the boundaries, can be considered as diffusion-unrestricted (the fast-diffusing pool); the local magnetization of this pool is uniform (with $\mathrm{Re}\,M \simeq \exp(-bD_0)$ and $\mathrm{Im}\,M \simeq 0$). The other population, comprising spins located near the boundaries, is diffusion-restricted due to encounters with the boundaries (the slow-diffusion pool). Although the magnetization of this pool is non-uniform, the presence of the sharp maxima allows one to describe a contribution of this pool to the total signal by means of a net ADC $D_1 < D_0$.

A similar situation takes place in the system with permeable boundaries. In Table 1, we provide the results of fitting the net signal in our periodic model (as a function of b-value in the interval $b \in [0,2]$), calculated by means of Eq. (19), to the function (31) for different $\tilde{\mu}$ at short diffusion time, $\tau = 0.01$ (at fixed time, the b-value is varied by changing the gradient strength G). Fitting parameters are D_1, D_2, and ζ. The bi-exponential function (31) fits the signal $S(b)$ extraordinarily well: $\chi^2 < 10^{-9}$.

As we see from Table 1, as permeability increases, the ADC D_2 corresponding to the fast-diffusion pool tends to the free-diffusion coefficient D_0, whereas the "population fraction" of the slow-diffusion pool ζ decreases because the exchange of spins across the

Table 1
Fit of the net signal $S(b)$ to the bi-exponential function (31) in the interval $\tilde{b} \in [0,2]$ ($\tau = 0.01$)

$\tilde{\mu}$	0	0.1	0.5	2.0	20
D_1/D_0	0.260	0.264	0.271	0.296	0.431
D_2/D_0	0.912	0.913	0.916	0.925	0.968
ζ	0.096	0.095	0.088	0.069	0.013

boundaries "nibbles" the slow-diffusing pool, decreasing the maxima and, consequently, decreasing ζ. The ADC D_1 tends to some constant value determined only by b-value and permeability μ and independent of the compartment size a, because spins located near one boundary do not encounter any other boundary at $t \ll t_D$.

Table 1 illustrates bi-exponential modeling of the net signal at short diffusion time $\tau = 0.01$. As diffusion time increases and the maxima in the real part of the local magnetization progressively decrease, the "population fraction" ζ of the slow-diffusion compartment decreases. In the case of impermeable boundaries, for sufficiently long time, when the local magnetization distribution is smooth, the concept of a division of the system into two components (pools) or two "quasi-compartments" becomes meaningless and a bi-exponential model fails [2]. However, as we will demonstrate below, in the system with permeable boundaries, bi-exponential modeling of the signal is possible in the long-diffusion time regime as well.

3.2. Long-diffusion time regime

In the long-diffusion time regime, $\tau \gg 1$, the time dependence of the net signal is mainly determined by the minimal root $k_{\min}$ of Eq. (20). According to Eqs. (21) and (22), this minimal root varies from 0 for $\tilde{\mu} = 0$ to $\tilde{q}(1 - (2\tilde{\mu})^{-1})$ for $\tilde{\mu} \gg 1$. The dependence of $k_{\min}$ on the reduced permeability $\tilde{\mu}$ is shown in Fig. 3 for different values of the parameter $\tilde{q}$.

For completely impermeable boundaries, the signal tends to a constant (in time); its q-dependence is described by the well-known sinc-function [29]:

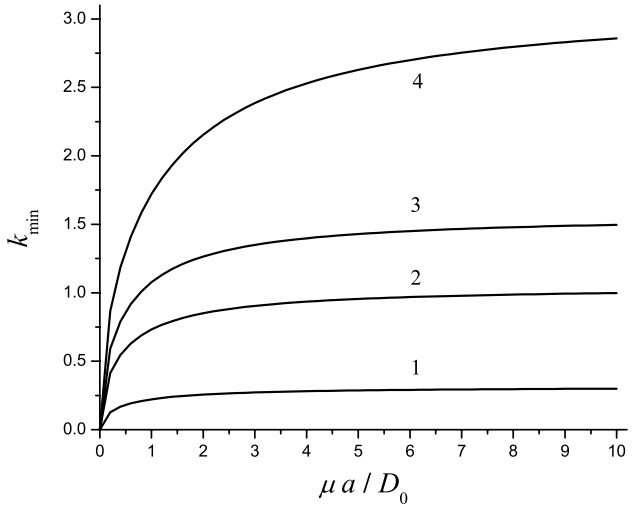

Fig. 3. The minimal root $k_{\min}$ of Eq. (20) as a function of the reduced permeability $\tilde{\mu} = \mu a/D_0$ at different values of the parameter $\tilde{q} = qa$: 1, $\tilde{q} = \pi/10$; 2, $\tilde{q} = \pi/3$; 3, $\tilde{q} = \pi/2$; and 4, $\tilde{q} = \pi$.

$$S(t) \to \mathrm{sinc}^2\left(\frac{qa}{2}\right) = \left[\frac{\sin(qa/2)}{(qa/2)}\right]^2. \tag{32}$$

However, for any $\tilde{\mu} \neq 0$, it is not so: at $t \gg t_D$, the signal mono-exponentially tends to 0, $S(t) \sim \exp(-\Gamma t)$ with the rate constant $\Gamma = D_0 k_{\min}^2/a^2$. In particular, for the case of small permeability, $\tilde{\mu} \ll 1$, Eq. (32) is modified as

$$S(t) \simeq \mathrm{sinc}^2\left(\frac{qa}{2}\right) \exp\left(-4\sin^2(qa/2)\frac{t}{t_\mu}\right), \quad t_\mu = \frac{a}{\mu}. \tag{33}$$

In fact, Eq. (33) is valid not only at $t \gg t_D$ but under "softer" condition $t > t_D$. In the case $qa \ll 1$, the signal (33) can be re-written as a mono-exponential function of b-value:

$$S \simeq \exp(-b\overline{D}), \quad \overline{D} = a\mu + \frac{a^2}{12t}. \tag{34}$$

At $t \gg t_D$, the phases of all spins within a single compartment have become identical (motional narrowing regime) and the net signal decay is completely determined by a slow (proportional to the permeability μ) spin exchange between adjacent compartments. Indeed, expression (33) represents a one-dimensional analog of the multi-site exchange approach developed by Callaghan [20, Chapter 7] (see also the pore-to-pore hopping model [22]).

For the case of high permeability, $\tilde{\mu} \gg 1$, the long-time behavior is mainly determined by diffusion and is similar to Eq. (23):

$$S(t) \simeq \exp[-b\overline{D}], \quad \overline{D} = D_0(1 - \tilde{\mu}^{-1}). \tag{35}$$

Although Eq. (35) is obtained under condition $\tau \gg 1$, a comparison with a numerical calculation shows that for $\tilde{\mu} > 10$, Eq. (35) provides an excellent approximation for the signal at arbitrary diffusion time t. For an arbitrary permeability μ, an analytical expression for the minimal root $k_{\min}$ of Eq. (20) is, generally, unavailable. However, it can be easily found in the case $\tilde{q} \ll 1$,

$$k_{\min} \simeq \tilde{q}\left(\frac{\tilde{\mu}}{\tilde{\mu}+1}\right)^{1/2} \tag{36}$$

and, consequently,

$$S(t) \simeq \exp[-b\overline{D}], \quad \overline{D} = D_0\frac{\tilde{\mu}}{\tilde{\mu}+1} = D_0\frac{\mu a}{\mu a + D_0}. \tag{37}$$

This limiting expression for the ADC $\overline{D}$ at long diffusion time and $q \to 0$ was found by Tanner [11]. For the case of steady-state diffusion between two distant points of a system such as ours, a similar relationship between D_0 and an overall diffusion coefficient $\overline{D}$ was also noted by Crick [30].

Thus, in the long-diffusion time regime and under condition $qa \ll 1$, the signal depends on the parameter q and time t only in the combination $b = q^2 t$ and can be approximated by a mono-exponential in the b-value

function (with some ADC $\overline{D}$ depending on a particular case). Obviously, this is not the case for arbitrary qa because the net signal, in general, depends on q and t in more complicated combinations (or does not depend on t at all, as in Eq. (32)). However, one can introduce the b-value in any case by a formal substitution $q = (b/t)^{1/2}$ and consider the signal as a function of b at fixed diffusion time t. In fact, this procedure has been already used when analyzing the bi-exponential modeling of the signal in the short-diffusion time regime. In this connection, a question arises which is motivated by numerous analyses of MR diffusion data from intact biological systems: is it possible to approximate the signal in the long-diffusion time regime by the bi-exponential function S_b, Eq. (31)? In the case of impermeable boundaries, when the signal in the long-time regime is described by the *sinc*-function expression (32), the answer is negative, however, for $\mu \neq 0$ the answer is positive, provided that the permeability is high enough (see a criterion below). In Table 2, we provide results of bi-exponential modeling of the signal at $t = 2t_D$ in the interval $\tilde{b} \in [0, 2]$ ($\chi^2 < 10^{-9}$).

For impermeable boundaries, $\mu = 0$, the signal in the interval $b \in [0, 2]$ is mono-exponential in the b-value with a low ADC ($0.043D_0$), that is rather close to the value $D_0/24$ predicted by Eq. (34). For non-zero permeability, a bi-exponential model well describes the net signal. With increase in permeability, both the parameters D_1 and D_2 increase, whereas the "population fraction" ζ of the slow-diffusion term tends to 0 and in the limit of free diffusion, $\mu = \infty$, the signal becomes mono-exponential with $D_2 = D_0$, as expected.

To explain, why a bi-exponential model is possible for $\mu \neq 0$ and fails for $\mu = 0$, in Fig. 4 we plot the quantity $\ln S$ as a function of $\tilde{b}$ at fixed diffusion time, $\tau = t/t_D = 2$, corresponding to the case of impermeable boundaries (solid line 1) and to the case of permeable boundaries with $\tilde{\mu} = 0.1$ (solid line 2). The dotted line corresponding to the mono-exponential approximation for $\mu = 0$ is valid only for $\tilde{b} < 10$ and fails for larger $\tilde{b}$. The dashed line corresponds well to the bi-exponential approximation (31) for $\tilde{\mu} = 0.1$ in the interval $\tilde{b} \in [0, 30]$ (fitting parameters: $\zeta = 0.36$, $D_1/D_0 = 0.04$, $D_2/D_0 = 0.19$).

As we see in Fig. 4, in the system with finite permeability, there is an interval of b-values, when the signal in the motional narrowing regime can be approximated by the bi-exponential function S_b (31). In the case of impermeable boundaries, such an interval is absent. There is an important difference between solid lines 1 and 2: a curvature of the former is negative, $\partial^2(\ln S)/\partial\tilde{b}^2 < 0$, whereas that of the latter is positive in the certain interval of b-value. For the bi-exponential function S_b, Eq. (31), the curvature of $\ln S_b$ is always positive, $\partial^2(\ln S_b)/\partial\tilde{b}^2 > 0$. That is why it is not possible to approximate line 1 by a bi-exponential function. Whereas line 2 allows such an approximation within the interval of the b-value in which its curvature is positive, $\partial^2(\ln S)/\partial\tilde{b}^2 > 0$. This interval substantially depends on the permeability and exists only if μ exceeds some critical value, μ_c. The latter can be found by equating $[\partial^2(\ln S)/\partial\tilde{b}^2]_{\tilde{b}=0}$ to 0. As a result, we get

$$\tilde{\mu}_c = \frac{1}{120\,\tau} \quad \text{or} \quad \mu_c = \frac{a}{120\,t}. \tag{38}$$

It is important to emphasize that in the long-diffusion time regime ($\tau > 1$), the local magnetization is practically uniform and, in contrast to the short-diffusion time regime, there is no physical interpretation of the model parameters as corresponding to two pools (quasi-compartments). Moreover, values of model parameters substantially depend on the interval of b-values over which the analysis is made.

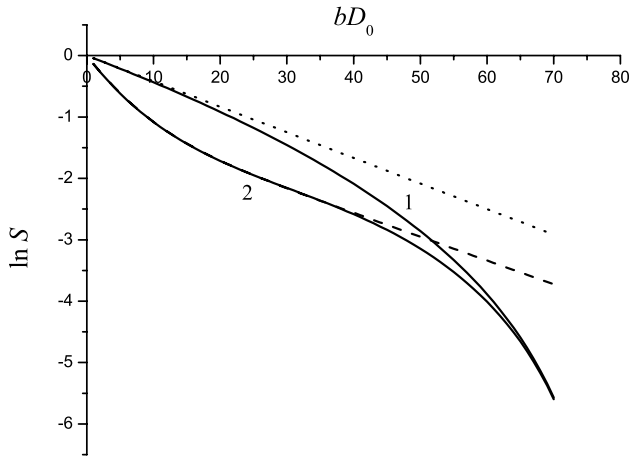

Fig. 4. The dependence of $\ln S$ on the reduced b-value $\tilde{b} = bD_0$ in the motional narrowing regime. Diffusion time is fixed, $\tau = t/t_D = 2$. Line 1, $\mu = 0$; line 2, $\mu = 0.1$; dotted line, mono-exponential approximation of S for $\mu = 0$; dashed line, bi-exponential approximation (31) of S for $\mu = 0.1$.

Table 2
Modeling of the net signal $S(b)$ by the bi-exponential function (31) in the interval $\tilde{b} \in [0, 2]$ ($\tau = 2$)

$\tilde{\mu}$	0	0.1	0.5	2.0	20
D_1/D_0	—	0.060	0.207	0.518	0.773
D_2/D_0	0.043	0.204	0.426	0.708	0.954
ζ	—	0.547	0.340	0.194	0.005

3.3. q-Space consideration

So far, we discussed the signal as a function of the parameter q, diffusion time t, or b-value. It is also well known that the Fourier transformation of the signal S with respect to the parameter q (q-space imaging) gives the so-called averaged diffusion propagator $\overline{P}(x, t)$ [20]:

$$\overline{P}(x, t) = \frac{1}{2\pi}\int_{-\infty}^{\infty} dq\, S \exp(iqx), \tag{39}$$

which determines a probability for a particle to diffuse a distance x during diffusion time t, averaged over the initial positions of the spins, x_0. For the periodic structure under consideration,

$$\overline{P}(x,t) = \frac{1}{a}\int_0^a \mathrm{d}x_0\, P(x_0+x,x_0,t). \tag{40}$$

For free diffusion, $\overline{P}(x,t)$ is Gaussian, $\overline{P}(x,t) = (4\pi D_0 t)^{-1/2}\exp(-x^2/4D_0 t)$. In the cases, when the signal's q-dependence is mono-exponential in q^2 (like in Eqs. (34), (35), and (37)), $\overline{P}(x,t)$ is also Gaussian with the corresponding ADC $\overline{D}$ rather than D_0. In the general case, the function $\overline{P}(x,t)$ has a more complicated structure providing information on a system's geometry [20,29]. The average propagator $\overline{P}(x,t)$ can be readily calculated in the case $\tau > 1$ and $\tilde{\mu} \ll 1$, when the signal is described by Eq. (33). Expanding the exponent in Eq. (33) in series of the modified Bessel functions I_n, we obtain

$$\begin{aligned} \overline{P}(x,t) &= \sum_{n=0}^{\infty}\eta_n(\beta)u(x-na), \\ \eta_n(\beta) &= \exp(-\beta)I_n(\beta), \end{aligned} \tag{41}$$

where $\beta = 2\mu t/a$ and $u(x)$ is the well-known Fourier transform of $\mathrm{sinc}^2(aq/2)$, describing the averaged propagator in the case of impermeable boundaries [29],

$$u(x) = (|x+a| + |x-a| - 2|x|)/2. \tag{42}$$

In the case of impermeable boundaries, only the term with $n = 0$ contributes to Eq. (41) and the function $\overline{P}(x,t)$ has the well-known triangle form described by Eq. (42) and is equal to 0 outside the interval $|x| \leqslant a$. In the case of finite permeability, it is a piecewise linear function of the displacement x, only two terms in the sum (nth and $(n+1)$th) contributing to $\overline{P}(x,t)$ within the interval $na < |x| < (n+1)a$. A spatial distribution of the average propagator $\overline{P}(x,t)$ is shown in Fig. 5 for two values of the parameter β: $\beta = 0$ (line 1) and $\beta = 0.5$ (line 2).

It is important to note that the line 2 in Fig. 5 creates the deceiving appearance of a multi-compartment system with different compartment sizes, while it actually reflects the permeable nature of boundaries in a multi-compartment system with a single compartment size.

The structure of the average propagator (41) allows a rather simple physical interpretation. Although in the motional narrowing regime, $\tau > 1$, where the spins' spatial distribution is uniform and there exists no *spatially* distinct pools (in contrast to the short-diffusion time regime), there exists an *implicit* differentiation of diffusing spins. All the spins can be conditionally divided into populations discriminated by the average displacement traveled during diffusion time t. One group of spins travels a distance less than the compartment size a, the relative population of spins—"weight"—of this group is

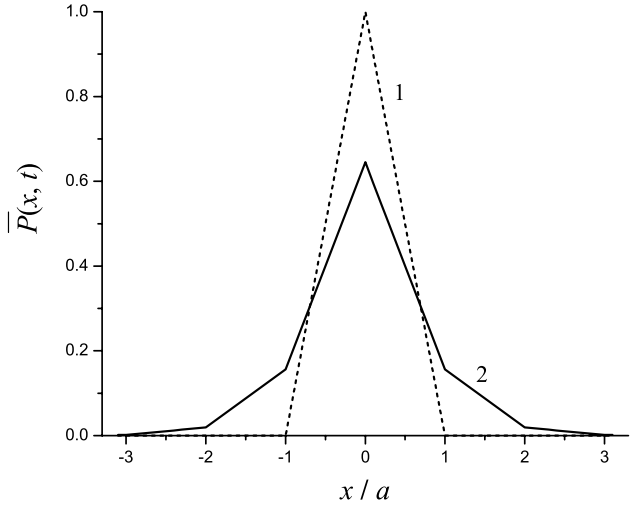

Fig. 5. The average propagator $\overline{P}(x,t)$ for $\beta = 0$ (line 1, dashed), and for $\beta = 0.5$ (line 2, solid).

equal to $\eta_0(\beta) = \exp(-\beta)I_0(\beta)$. A second group comprises spins that travel distances longer than a but less than $2a$, its "weight" is $\eta_1(\beta)$, and so on. In the case of impermeable boundaries, $\beta = 0$, only the first group of spins contributes to the sum in Eq. (41) because $I_n(\beta) \sim \beta^n$, and $\overline{P}(x,t) = u(x)$. For barely permeable boundaries, $\beta \ll 1$, when only linear terms in β are taken into account, $\eta_1(\beta) \sim \beta \neq 0$, and the second group of spins becomes "visible"; accounting for terms proportional to β^2 makes the third group "visible" with $n = 2$, etc. Line 2 in Fig. 5 corresponds to a rather small value of $\beta = 0.5$, and therefore the average propagator rapidly decreases with x (in Fig. 5 only the contributions of first three terms are "visible"). As the parameter β increases, the central maximum $\overline{P}(0,t)$ decreases whereas the width of $\overline{P}(x,t)$ increases. In the limit $\beta \gg 1$

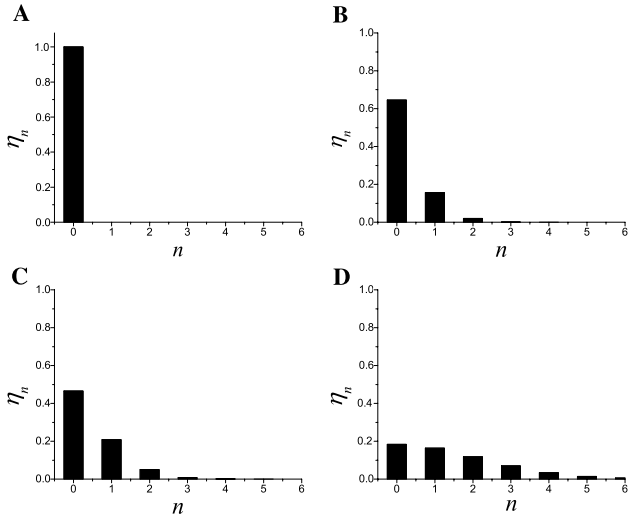

Fig. 6. The relative populations of spins in the groups ("weights"), η_n, for different values of the parameter $\beta = 2\mu t/a$. (A) $\beta = 0$; (B) $\beta = 0.5$; (C) $\beta = 1$; and (D) $\beta = 5$.

(very long diffusion time), it can be approximated by the Gaussian envelope,

$$\overline{P}(x,t) \simeq (4\pi\overline{D}t)^{-1/2}\exp(-x^2/4\overline{D}t), \quad \overline{D} = \mu a, \qquad (43)$$

though the piecewise linear structure of $\overline{P}(x,t)$ holds for any β. For better illustration, in Fig. 6 we present not the average propagator itself but a histogram of the "weights" corresponding to different groups.

As mentioned above, at $\beta = 0$ (impermeable boundaries) only the first group of spins exists. As β increases, "weights" of groups with $n \neq 0$ increase, in essence, the presence of permeable boundaries has "discretized" the spin population vis-à-vis displacement distance; at $\beta \gg 1$, the envelope characterizing the relative populations is described by the Gaussian function (43).

4. Conclusion

In the present paper, the local magnetization distribution $M(x,t)$ and the net MR signal S arising from a one-dimensional periodic structure with permeable barriers in a Tanner–Stejskal pulsed-field gradient experiment are considered. In the framework of the narrow pulse approximation, the general expressions for $M(x,t)$ and S as functions of diffusion time t and the parameter $q = \gamma G\delta$ are obtained and analyzed. The real part of the local magnetization is shown to be continuous at the boundaries whereas the imaginary part is discontinuous. At short diffusion times, $t \ll t_D$, the local magnetization is strongly spatially inhomogeneous and has the maxima in the vicinity of the boundaries, the amplitudes of these maxima depending on barrier permeability. The net signal as a function of the b-value at constant diffusion time is well approximated in the short-diffusion time regime by a bi-exponential function with a clear physical interpretation of the model parameters as the ADCs and "population fractions" of the slow- and fast-diffusing quasi-compartments (pools). The bi-exponential (in b-value) behavior of the signal in a single-compartment system with impermeable boundaries can be observed at $t < 0.02\,t_D$, that implies an upper limit for the diffusion time. Let us take the observed water diffusion coefficient in biological systems $\sim$1 μm^2/ms as a lower limit on the "free"-diffusion coefficient D_0 for intracellular water. For a cell size $a \sim$1 μm, the characteristic diffusion time is then $t_D \sim 1$ ms. For typical cell membrane, $\mu \sim 10^{-2}$–10^{-3} cm/s, this condition remains practically the same. Thus, bi-exponential signal behavior due to the inhomogeneous magnetization distribution in the short-diffusion time regime can be observed in cells with $a \sim 1$ μm only at extremely short diffusion time, $t < 0.02$ ms. Alternatively, for a typical diffusion time $t \sim 10$ ms, only much larger cells with $a \sim 25$ μm ($t_D \sim 600$ ms) or greater would reveal the short-time bi-exponential net signal behavior.

In the long-diffusion time regime, $t > t_D$, the net signal from our multi-compartment system with permeable boundaries is mono-exponential as a function of diffusion time at constant q but has a more complicated structure as a function of q^2 at constant t. In contrast to systems with impermeable boundaries, the signal in the long-diffusion time regime can also be well approximated by a bi-exponential function. Such a quasi-bi-exponential behavior of the signal in the long-diffusion time regime can be observed when the condition $\mu > \mu_c$ (see Eq. (38)) is met. This implies a lower limit on the diffusion time t. For $\mu \sim 10^{-2}$–10^{-3} cm/s and cells with $a \sim 1$ μm, the condition $\mu > \mu_c$ is met for the diffusion time $t > 1$ ms. The long-diffusion time regime holds for such cells at $t > t_D \sim 1$ ms. Consequently, the bi-exponential behavior of the signal, caused by finite membrane permeability, can be observed at typical experimental diffusion times (10 ms and longer).

Hence, bi-exponential behavior of the signal, arising from the above-elucidated considerations, can be expected in biological cells with permeable membranes in both the short- and long-diffusion time regimes. In the short-diffusion time regime, the physical origin of "bi-exponentiality" is the same as in the one-compartment model with impermeable boundaries, an inhomogeneous distribution of the transverse magnetization. However, in the long-diffusion time regime, the permeability of the boundaries plays the major role in defining bi-exponential signal behavior. Obviously, this bi-exponential behavior cannot be interpreted as resulting from two distinct physical compartments. This mechanism of "bi-exponentiality" of the signal should be taken into account when interpreting experimental results.

The average propagator $\overline{P}(x,t)$ obtained in the case $t > t_D$, $\tilde{\mu} \ll 1$ by means of Fourier transformation of the signal with respect to q reveals an implicit discrete discrimination of spin populations by distance traveled during time t. The structure of $\overline{P}(x,t)$ in this regime creates the deceiving appearance of a multi-compartment system with different compartment sizes. In actuality, this structure reflects the permeable nature of boundaries in a multi-compartment system with a single compartment size. This effect should be also taken into account for correct interpretation of experimental data derived by q-space imaging procedures on systems with permeable boundaries.

Acknowledgments

This work is supported in part by NIH Grants R01-NS41519, R01-HL70037, and R24-CA83060 (NCI Small Animal Imaging Resource Program (SAIRP)) and P30 CA91842 (NCI Cancer Center Support Program).

Appendix A

The net signal (per unit length) $S(t)$ and the local magnetization distribution at the boundaries $M(x=0,t)$ in the short-diffusion time regime, $t \ll t_D$, are given by the inverse Laplace transformation of Eqs. (27) and (29), respectively.

$$S(t) = \exp(-\tilde{q}^2\tau) + \frac{1}{(4\tilde{\mu}^2+\tilde{q}^2)^2} I_1(\tilde{q},\tilde{\mu},\tau) + \frac{1}{(4\tilde{\mu}^2+\tilde{q}^2)} I_2(\tilde{q},\tilde{\mu},\tau), \tag{A.1}$$

$$M(x=0,t) = \exp(-\tilde{q}^2\tau) + \mathrm{i}\tilde{q} I_1(\tilde{q},\tilde{\mu},\tau), \tag{A.2}$$

$$\begin{aligned} I_1(\tilde{q},\tilde{\mu},\tau) &= \exp(-\tilde{q}^2\tau)[2\tilde{\mu} + \tilde{q}\Phi_i(\tilde{q}\tau^{1/2})] \\ &\quad - 2\tilde{\mu}\exp(4\tilde{\mu}^2\tau)\tilde{\Phi}(2\tilde{\mu}\tau^{1/2}), \\ I_2(\tilde{q},\tilde{\mu},\tau) &= 2\tilde{\mu}\tau\exp(-\tilde{q}^2\tau) - (\tau/\pi)^{1/2} \\ &\quad + \exp(-\tilde{q}^2\tau)(\tilde{q}\tau - 1/2\tilde{q})\Phi_i(\tilde{q}\tau^{1/2}). \end{aligned} \tag{A.3}$$

Here $\tilde{\Phi}(x) = 1 - \Phi(x)$, $\Phi_i(x) = \Phi(ix)/i$, $\Phi(x)$ is the error function (e.g. [31]).

References

[1] MR and Order in Biological Tissue. Issue Edited by Chris Boesch, NMR Biomed. 14 (2001).

[2] A. Sukstanskii, J.J.H. Ackerman, D. Yablonskiy, Effects of barrier-induced nuclear spin magnetization inhomogeneities on diffusion-attenuated MR signal, Magn. Reson. Med. 55 (2003) 735.

[3] C. Beaulieu, P.S. Allen, Water diffusion in the giant axon of the squid: implications for diffusion-weighted MRI of the nervous system, Magn. Reson. Med. 32 (1994) 579.

[4] D. Le Bihan, P. Van Zijl, From the diffusion coefficient to the diffusion tensor, NMR Biomed. 15 (2002) 431.

[5] S.N. Hwang, C.L. Chin, F.W. Wehrli, D.B. Hackney, An image-based finite difference model for simulating restricted diffusion, Magn. Reson. Med. (2003).

[6] D.A. Yablonskiy, G.L. Bretthorst, J.J. Ackerman, Statistical model for diffusion attenuated MR signal, Magn. Reson. Med. 50 (2003) 664.

[7] A. Schwarcz, P. Bogner, P. Meric, J.-L. Correze, Z. Berente, J. Pal, F. Gallyas, T. Doczi, B. Gillet, J.-C. Beloeil, The existence of biexponential signal decay in magnetic resonance diffusion-weighted imaging appears to be independent of compartmentalization, Magn. Reson. Med. 51 (2004) 278.

[8] A.L. Sukstanskii, D.A. Yablonskiy, Effects of restricted diffusion on MR signal formation, J. Magn. Reson. 157 (2002) 92.

[9] H.C. Torrey, Bloch equations with diffusion terms, Phys. Rev. 104 (1956) 563.

[10] S.D. Stoller, W. Happer, F.J. Dyson, Transverse spin relaxation in inhomogeneous magnetic field, Phys. Rev. A 44 (1991) 7459.

[11] J.E. Tanner, Transient diffusion in a system partitioned by permeable barriers. Application to NMR measurements with a pulsed field gradient, J. Chem. Phys. 69 (1978) 1748.

[12] A.V. Barzykin, K. Hayamizu, W.S. Price, M. Tachia, Pulsed-field-gradient NMR of diffusive transport through a spherical interface into a external medium containing a relaxation agent, J. Magn. Reson. Ser. A 114 (1995) 39.

[13] W.S. Price, A.V. Barzykin, K. Hayamizu, M. Tachia, A model for diffusive transport through a spherical interface probed by pulsed-field gradient NMR, Biophys. J. 74 (1998) 2259.

[14] A. Szafer, J. Zhong, J.C. Gore, Theoretical model for water diffusion in tissues, Magn. Reson. Med. 33 (1995) 697.

[15] D.S. Novikov, D. van Dusschoten, H. van As, Modeling of self-diffusion and relaxation time NMR in multi-compartment systems, J. Magn. Reson. 135 (1998) 522.

[16] C.L. Chin, F.W. Wehrli, S.N. Hwang, M. Takahashi, D.B. Hackney, Biexponential diffusion attenuation in the rat spinal cord: computer simulations based on anatomic images of axonal architecture, Magn. Reson. Med. 47 (2002) 455.

[17] L. van der Weerd, S.M. Melnikov, F.J. Vergeldt, E.G. Novikov, H. van As, Modelling of self-diffusion and relaxation time NMR in multicompartment systems with cylindrical geometry, J. Magn. Reson. 156 (2002) 213.

[18] J. Kärger, Zur bestimmung der diffusion in einem zweibereich-system mit hilfe von gepulsten fieldgradienten, Ann. Phys. 24 (1969) 1.

[19] J. Andrasko, Water diffusion permeability of human erythrocytes studied by a pulsed gradient NMR technique, Biochim. Biophys. Acta 428 (1976) 304.

[20] P.T. Callaghan, Principles of Nuclear Magnetic Resonance Microscopy, Claredon Press, Oxford, NY, 1991.

[21] G.J. Stanisz, A. Szafer, G.A. Wright, R.M. Henkelman, An analytical model of restricted diffusion in bovine optic nerve, Magn. Reson. Med. 37 (1997) 103.

[22] P.C. Jiang, T.Y. Yu, W.C. Perng, L.P. Hwang, Pore-to-Pore hopping model for the interpretation of the pulsed gradient spin echo attenuation of water diffusion in cell suspension systems, Biophys. J. 80 (2001) 2493.

[23] J.H. Lee, C.S. Springer, Effects of equilibrium exchange on diffusion-weighted NMR signals: the diffusigraphic "shutter-speed", Magn. Reson. Med. 49 (2003) 450.

[24] L.L. Latour, K. Svoboda, P.P. Mitra, C.H. Sotak, Time-dependent diffusion of water in a biological model system, Proc. Natl. Acad. Sci. USA 91 (1994) 1229.

[25] P.P. Mitra, P.N. Sen, L.M. Schwartz, Short-time behavior of the diffusion coefficient as a geometrical probe of porous media, Phys. Rev. B 47 (1993) 8565.

[26] E.O. Stejskal, Use of spin echoes in a pulsed magnetic-field gradient to study anisotropic, restricted diffusion and flow, J. Chem. Phys. 43 (1965) 3597.

[27] E.O. Stejskal, J.E. Tanner, Spin diffusion measurements: spin echoes in the presence of a time-dependent field gradient, J. Chem. Phys. 42 (1965) 288.

[28] J.E. Tanner, E.O. Stejskal, Restricted self-diffusion of protons in colloidal systems by the pulsed-gradient, spin-echo method, J. Chem. Phys. 49 (1968) 1768.

[29] D.G. Cory, A.N. Garroway, Measurement of translational displacement probabilities by NMR: an indicator of compartmentation, Magn. Reson. Med. 14 (1990) 435.

[30] F. Crick, Diffusion in Embryogenesis, Nature 225 (1970) 420.

[31] I.S. Gradstein, I.M. Ryzhik, Table of Integrals, Series, and Products, Academic Press, New York, 1999.